Electronic Supplementary Information (ESI) for *"Formation of highly porous $CuCo_2O_4$ nanosheet assemblies for high-rate and long-term lithium storage"*

Jia Li[a], Yongxing Zhang[a*], Li Li[a], Lixun Cheng[a], Song Dai[a], Fei Wang[a], Yanming Wang[a] and Xin-Yao Yu[b,c*]

[a] Key Laboratory of Green and Precise Synthetic Chemistry and Application of, Ministry of Education, Huaibei Normal University

[b] Institutes of Physical Science and Information Technology, Anhui University, Hefei 230601, P. R. China

[c] School of Materials Science & Engineering, Zhejiang University, Hangzhou 310027, P. R. China

E-mail: zyx07157@mail.ustc.edu.cn; E-mail: yuxinyao@ahu.edu.cn

Experimental section

Synthesis of $CuCo_2O_4$ NSAs

In a typical procedure, 0.5 mmol of $Cu(CH_3COO)_2{\cdot}4H_2O$, 1 mmol of $Co(CH_3COO)_2{\cdot}4H_2O$ and 16 mmol urea were dissolved in a solution of 15 mL deionized water and 15 mL glycerol, follow on stirred at room temperature for 15 min, then added about 1 mmol Cetyltrimethyl Ammonium Bromide (CTAB), and continue stirring at room temperature until it form a transparent solution. The resulting solution was transferred into a capacity of 50 mL a Teflon-lined stainless autoclave and was kept at 140 °C for 10 h. After the autoclave was cooled to ambient temperature naturally, the pink precursor was obtained after centrifugation and washed with deionized water and ethanol for several times, and then the product was dried in a vacuum over at 60 °C for 12 h. And then, the as-prepared product was annealed at 450 °C under the air atmosphere for 3 h with a temperature ramp rate of 1 °C min^{-1} to obtain hierarchical porous $CuCo_2O_4$ nanosheet assemblies (denoted $CuCo_2O_4$ NSAs). The pink precursor was finally converted into the black powder. For comparison, uneven size $CuCo_2O_4$ microparticles (denoted as $CuCo_2O_4$ MPs) were prepared through a similar procedure without adding CTAB; The Co_3O_4 microcubes (denoted as $CuCo_2O_4$ MCs) were synthesized under the same condition except that only $Co(CH_3COO)_2{\cdot}4H_2O$ was used instead of the mixture of $Co(CH_3COO)_2{\cdot}4H_2O$ and $Cu(CH_3COO)_2{\cdot}4H_2O$.

Material characterization

X-ray diffraction (XRD) patterns were obtained in the 2θ range of 10-80° using a Philips X'Pert Pro X-ray diffractometer with Cu Kα radiation (1.5418 Å). Field emission scanning electron microscopy

(FESEM) images were taken on a FESEM (S-4800) operated at an accelerating voltage of 1.0 kV. Transmission electron microscopy (TEM) and high resolution transmission electron microscope (HRTEM) images were obtained on a JEOL JEM-2010 transmission electron microscope, equipped with X-ray energy dispersive spectroscopy (EDS) capabilities, working at an acceleration voltage of 200 kV. Thermogravimetric analysis was conducted on a TGA-2050 (TA Corp.) thermal analysis system under a heating rate of 5 °C min^{-1} from 20 to 800 °C with an air flow rate of 100 mL min^{-1}. The nitrogen adsorption-desorption isotherms and pore-size distributions of the as-prepared product were measured by Brunauer-Emmett-Teller (BET) and Barrett-Joyner-Halenda (BJH) methods (Micromeritics, ASAP2020M+C). And all the as-prepared products were degassed at 150 °C for 4 h prior to nitrogen adsorption survey.

Electrochemical measurements

The electrochemical performances of the three samples were investigated using CR2016-type coin cells with high purity lithium foil as the counter/reference electrode. The working electrodes were composed of the three samples active materials, Super P conductive carbon and polyvinylidene difluoride binder at a weight ratio of 70 : 20 : 10 in an N-methyl pyrrolidone solvent, which fully stirring. The mixture slurry was coated onto a current collector (Cu foil). After drying at 80 °C in a vacuum oven overnight, the current collector then was cut into a 12 mm disk as the working electrode, coated the three samples active materials with the mass of ~ 1.0 mg cm^{-2}. The cell was assembled in an argon-filled glovebox with Celgard 2400 membrane as the separator, and the electrolyte solution was formed by dissolving 1 M $LiPF_6$ in a mixture solvent of ethylene carbonate (EC), ethyl methyl carbonate (EMC) and dimethyl carbonate (DMC) (EC: EMC: DMC = 1: 1: 1 by volume) as the electrolyte. The galvanostatic charging-discharging cycles were measurements on a battery tester with a volatge window of 0.01~3.0 V vs. Li/Li^+ at various current densities. Cyclic voltammograms (CV, 0.1 mV s^{-1}) and electrochemical impedance spectra (EIS, 0.01-100 kHz) were both evaluated by a CHI760E electrochemical workstation. All electrochemical measurements were implemented at room temperature.

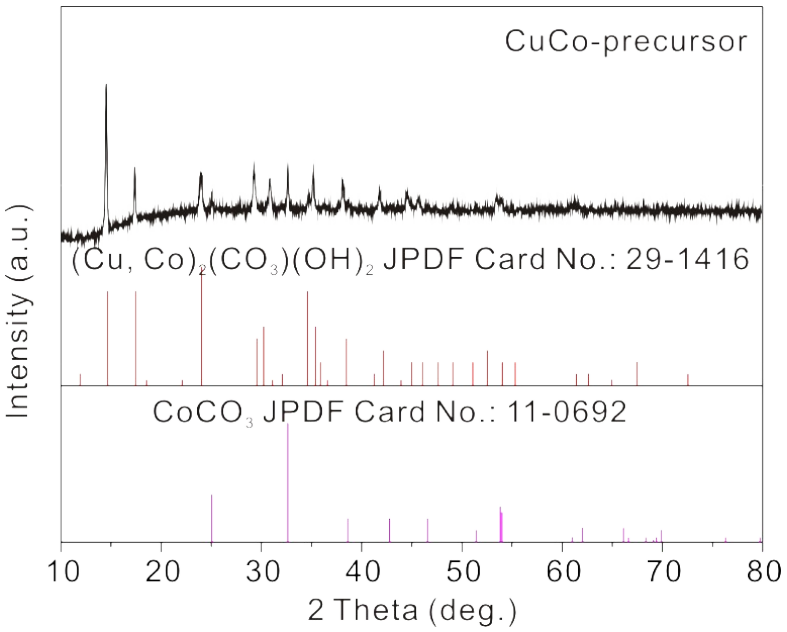

Fig. S1 XRD pattern of nanosheet-assembled CuCo-precursor

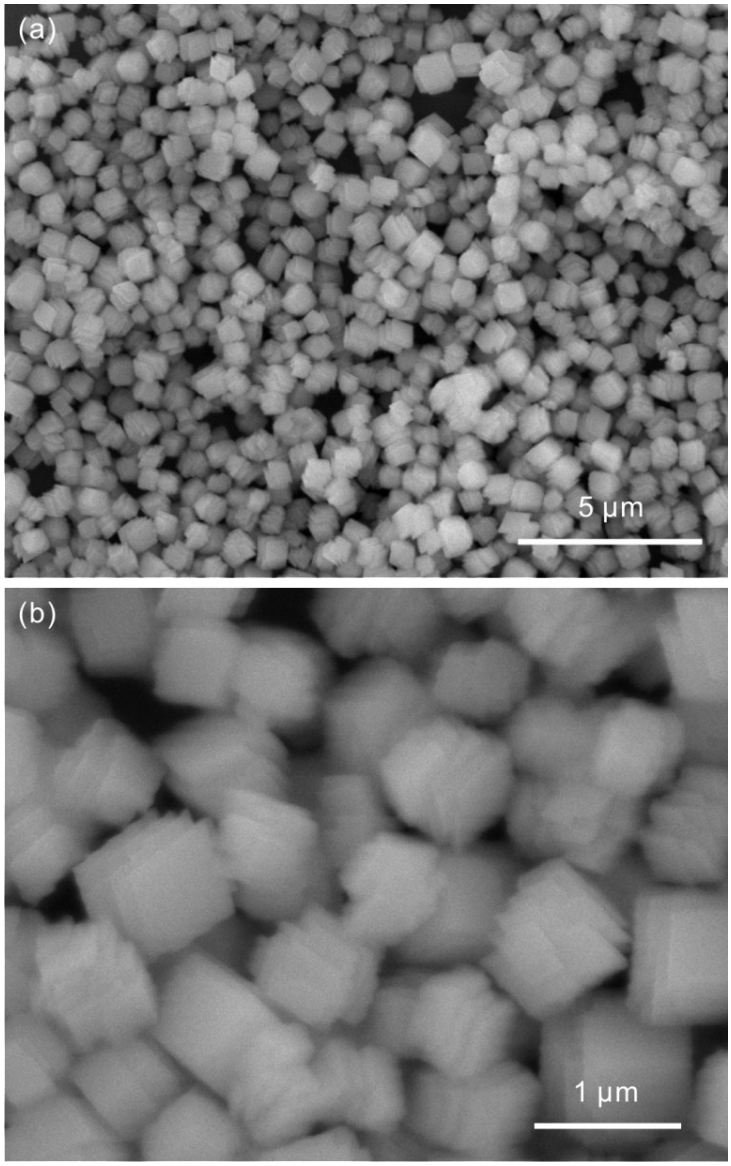

Fig. S2 (a) Low and (b) High magnification SEM images of the nanosheet-assembled CuCo-precursor

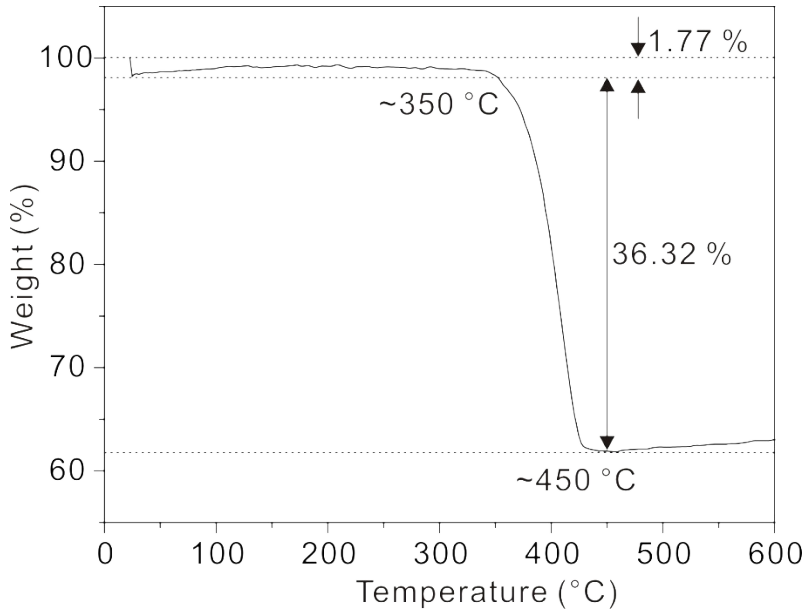

Fig. S3 TGA curves nanosheet-assembled CuCo-precursor in air with an increasing rate of 5 °C min^{-1}.

The product experiences a weight loss of 38.09 wt% in the temperature range between room temperature to 450 °C with a heating rate of 5 °C min^{-1}. The weight loss is about 1.77 wt% at ~ 350 °C because of the vaporization of physical and chemical adsorption of moisture, the adsorbed water and some organic species. The coming main weight loss (36.32 wt%) between 350 °C and 450 °C is due to the decomposition of nanosheet-assembled CuCo-precursors into $CuCo_2O_4$ NSAs.

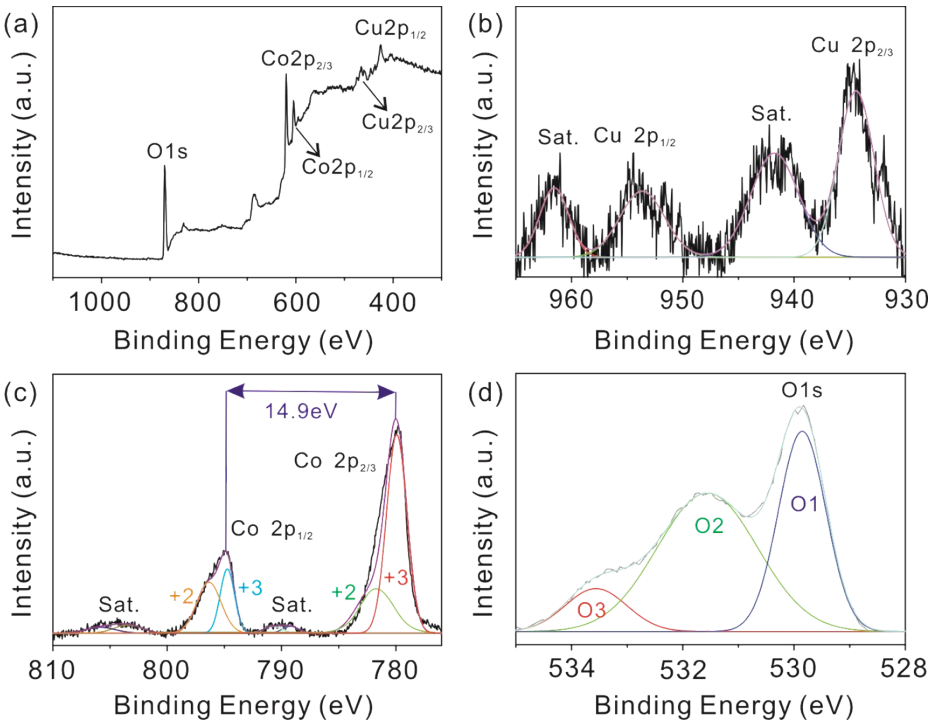

Fig. S4 XPS spectra of the $CuCo_2O_4$ NSAs: (a) survey spectrum and high-resolution, (b) Cu 2p, (c) Co 2p, and (d) O 1s.

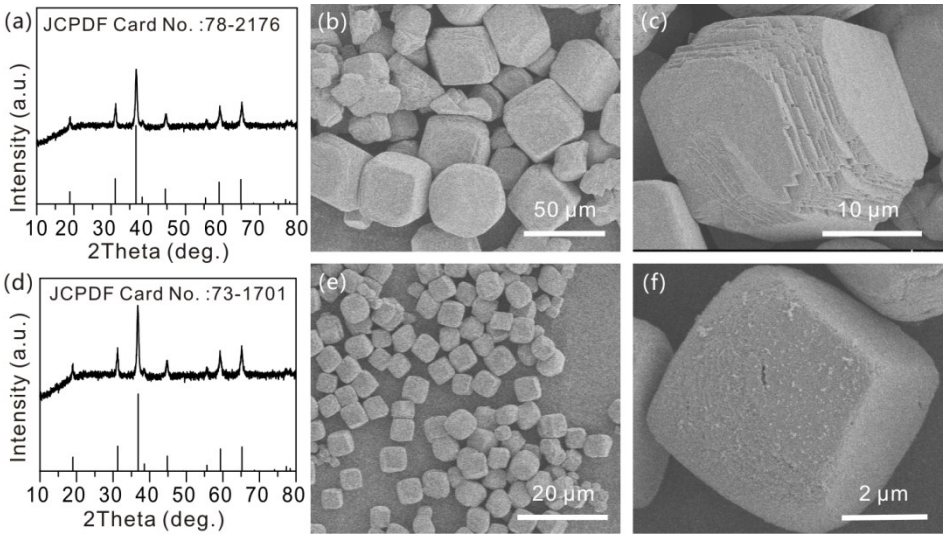

Fig. S5 XRD patterns of $CuCo_2O_4$ MPs (a) and Co_3O_4 MCs (d), SEM images of $CuCo_2O_4$ MPs (b-c) and Co_3O_4 MCs (e-f)

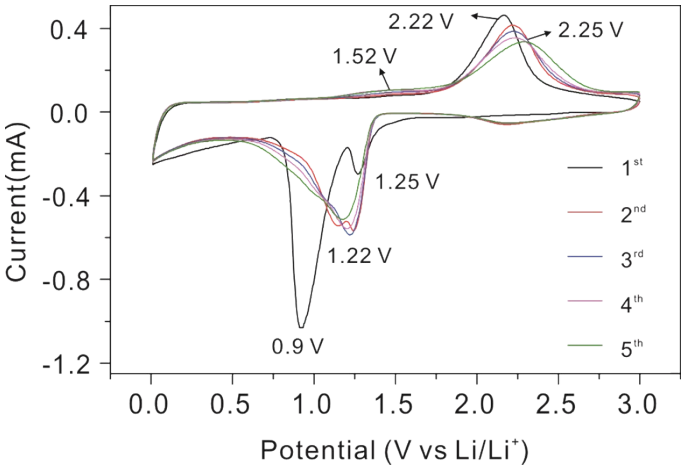

Fig. S6 CV curves for the initial five cycles at a scan rate of 0.1 mV s^{-1} in the voltage range of 0.01-3.0 V of $CuCo_2O_4$ NSAs electrode

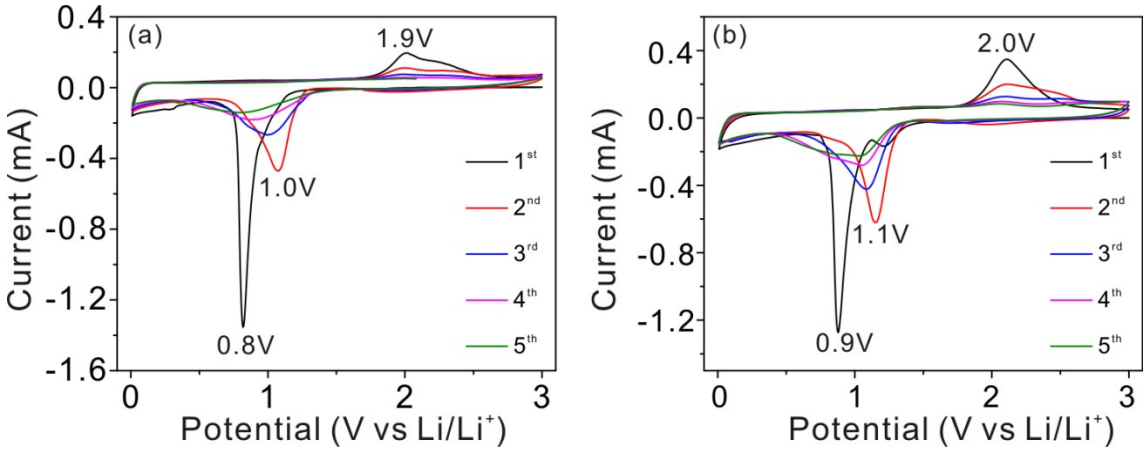

Fig. S7 CV curves for the initial five cycles at a scan rate of 0.1 mV s^{-1} in the voltage range of 0.01-3.0 V of (a) Co_3O_4 MCs and (b) $CuCo_2O_4$ MPs electrode

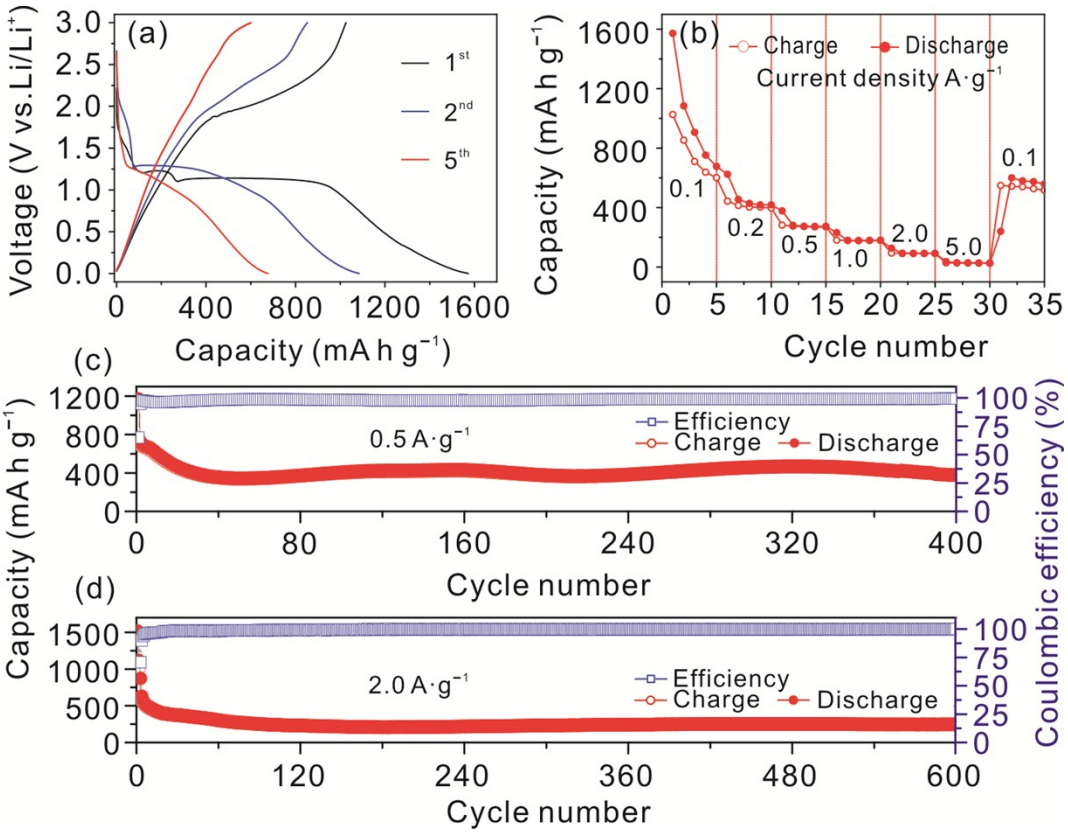

Fig. S8 (a) Typical discharge–charge voltage profiles of the Co_3O_4 MCs electrode at a current density of 0.1 A g^{-1} . (b) Rate performances of the Co_3O_4 MCs. (c) Cycling performances of the Co_3O_4 MCs electrodes at a current density of 0.5 and 2 A g^{-1}, respectively.

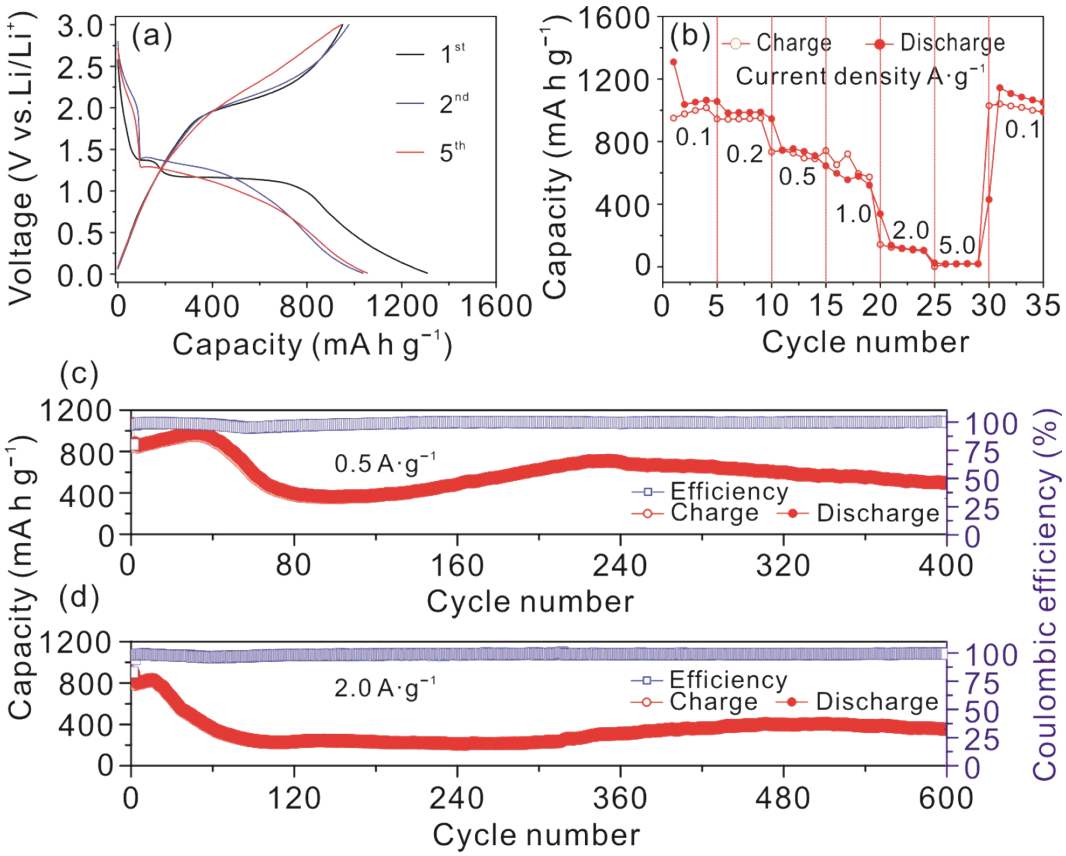

Fig. S9 (a) Typical discharge–charge voltage profiles of the $CuCo_2O_4$ MPs electrode at a current density of 0.1 A g^{-1} . (b) Rate performances of the $CuCo_2O_4$ MPs. (c) Cycling performances of the $CuCo_2O_4$ MPs electrodes at a current density of 0.5 and 2 A g^{-1}, respectively.

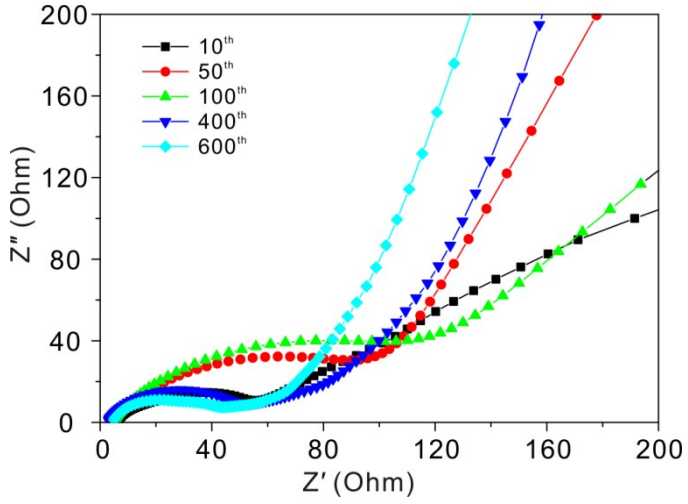

Fig. S10 Electrochemical impedance spectra (EIS) of the $CuCo_2O_4$ NSAs anode for different cycles at current density of 2 A g^{-1}.

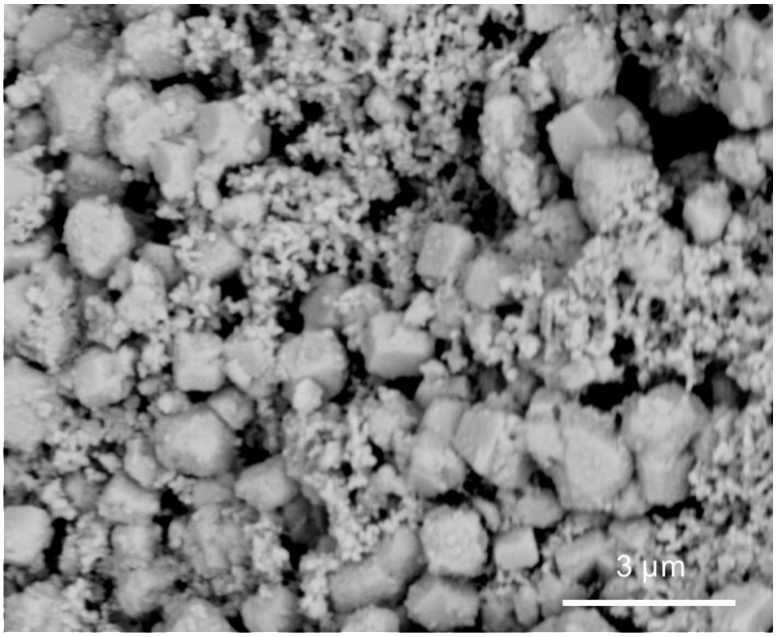

Fig. S11 SEM image of the $CuCo_2O_4$ NSAs constructed by porous nanosheets anode after cycling test

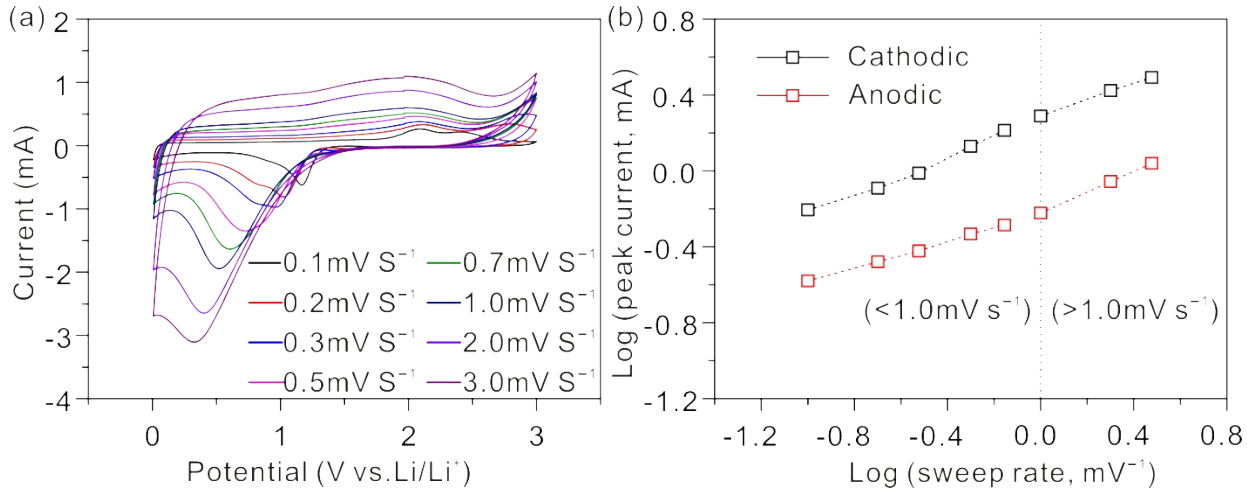

Fig. S12 (a) CV profiles of the $CuCo_2O_4$ NSAs at various scan rates ranging from 0.1 to 3.0 mV s^{-1}; (b) log(i) versus log(v) plot for the $CuCo_2O_4$ NSAs obtained from the CV data.

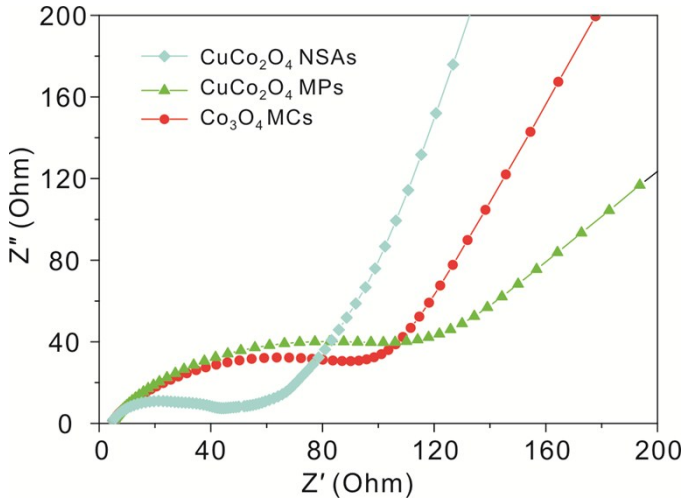

Fig. S13 Electrochemical impedance spectra (EIS) of the three anodes after cycling test at current density of 0.5 A g^{-1}.

Table S1 Comparison of electrochemical results for $CuCo_2O_4$–based anodes

$CuCo_2O_4$	Capacity(mAh g^{-1})/cycle number	**Current density (mA g^{-1})**	**Ref.**
$CuCo_2O_4$ nanocube	471.7/350th	2000	1
$CuCo_2O_4$ concave polyhedron	411/150th	1000	2
$CuCo_2O_4$ microsphere	800/120th	1000	3
$CuCo_2O_4$ microflower	612/500th	1000	4
$CuCo_2O_4$ nanofiber	610/800th	600	5
$CuCo_2O_4$ microsphere	635/100th	100	6
Porous $CuCo_2O_4$ nanosheet assemblies	**1302/400th**	**500**	**This work**
	1104/600th	**2000**	

References

1. W. Kang, Y. Tang, W. Li, Z. Li, X. Yang, J. Xu and C. S. Lee, *Nanoscale*, 2014, **6**, 6551-6556.
2. J. J. Ma, H. J. Wang, X. Yang, Y. Q. Chai and R. Yuan, *J. Mater. Chem. A*, 2015, **3**, 12038-12043.
3. J. Cheng, X. Li, Z. Wang, H. Guo, W. Peng and Q. Hu, *Ceram. Int.*, 2016, **42**, 2871-2875.
4. F. Niu, N. Wang, J. Yue, L. Chen, J. Yang and Y. Qian, *Electrochim. Acta*, 2016, **208**, 148-155.
5. H. Zhang, Z. Y. Tang, K. Zhang, L. Wang, H. M. Shi, G. H. Zhang and H. G. Duan, *Electrochim. Acta*, 2017, **247**, 692-700.
6. L. Lu, F. X. Min, Z. H. Luo, S. Q. Wang, F. Teng, G. H. Li and C. Q. Feng, *J. Nanosci. Nanotechnol.*, 2017, **17**, 4763-4771.